

P. PIETRUSIEWICZ*, M. NABIALEK*, M. SZOTA**, K. PERDUTA***

MICROSTRUCTURE AND SOFT MAGNETIC PROPERTIES OF $\text{Fe}_{61}\text{Co}_{10}\text{Y}_8\text{Me}_1\text{B}_{20}$ (WHERE Me =W, Zr or Nb) AMORPHOUS ALLOYS

STRUKTURA I WŁASNOŚCI MAGNETYCZNE STOPÓW AMORFICZNYCH $\text{Fe}_{61}\text{Co}_{10}\text{Y}_8\text{Me}_1\text{B}_{20}$ (M = W, Zr, Nb)

The microstructure and the soft magnetic properties of the multi-component $\text{Fe}_{61}\text{Co}_{10}\text{Y}_8\text{Me}_1\text{B}_{20}$ amorphous alloys (where Me = W, Zr or Nb) have been investigated; the samples were in the form of ribbons of 3 mm width and 30 μm thickness. The samples were produced using a single-roller melt-spinning method. The alloy composition was investigated using an X-ray diffractometer. The amorphous nature of the entire volume of all the as-quenched samples was confirmed. From the magnetic measurements performed using the 'LakeShore' vibrating sample magnetometer, magnetic parameters such as: coercivity, saturation of the magnetization for the as-quenched samples were derived. All of the investigated alloys displayed good soft magnetic properties, making them perfect materials for magnetic cores. The core losses for different values of magnetic field and operating frequency were also measured. It was shown that the investigated alloys featured lower core losses than commercially-used classical FeSi steel.

Keywords: magnetic properties, core losses, amorphous alloys, magnetic permeability

W pracy przedstawiono wyniki badań mikrostruktury i właściwości magnetycznych wieloskładnikowych stopów amorficznych o składach $\text{Fe}_{61}\text{Co}_{10}\text{Y}_8\text{Me}_1\text{B}_{20}$ (Me = W, Zr, Nb) w postaci taśm o szerokości 3 mm i grubości około 30 μm . Badane materiały otrzymano metodą szybkiego chłodzenia ciekłego stopu na wirującym walcu miedzianym. Za pomocą dyfraktometru rentgenowskiego zbadano strukturę wytworzonych materiałów. Z badań tych wynika, że otrzymane w stanie po zestaleniu próbki były w pełni amorficzne. Na podstawie przeprowadzonych pomiarów wykonanych przy użyciu magnetometru wibracyjnego określono wartość: pola koercji, magnetyzacji nasycenia. Straty energii na przemagnesowanie oraz maksymalną przenikalność magnetyczną wyznaczono przy zastosowaniu aparatury, w której wykorzystuje się metodę transformatorową. Pomiar wykonano w zmiennym polu magnetycznym i przy różnych częstotliwościach. Badania te wykazały, że wytworzone szkła metaliczne w stanie po zestaleniu cechują się znacznie mniejszymi stratami na przemagnesowanie niż klasyczne blachy transformatorowe FeSi.

1. Introduction

The multi-component amorphous alloys based on iron are very interesting due to their excellent soft magnetic properties, such as: high values of saturation of the magnetization and magnetic permeability and very low values of coercivity. Also, the core losses are much lower in comparison to classical FeSi transformer steels [1, 2]. The amorphous materials lack so-called magnetocrystalline anisotropy; this is typical for materials with a periodic structure of atoms. In crystalline materials, an increase in magnetocrystalline anisotropy results in a higher magnetic field required to saturate the material to saturation. In turn, this results in higher coercivity. This ex-

plains why the absence of magnetocrystalline anisotropy in the amorphous alloys generates their excellent soft magnetic properties, making them suitable for application in electrotechnical industry. These applications include: low-loss transformer cores, magnetic sensors and magnetic recording heads [3-6]. There are many methods for producing energetically unstable alloys which feature amorphous structure throughout their volume. One of the most common techniques is a single-roller melt-spinning method. In this method, the liquid material is ejected onto a copper wheel, and quenched at a rate of 10^4 – 10^6 K/s. The obtained samples are of ribbon form with thicknesses of less than 100 μm . Amorphous samples with thicknesses greater than this can be produced at much slower

* CZESTOCHOWA UNIVERSITY OF TECHNOLOGY, INSTITUTE OF PHYSICS, 42-200 CZĘSTOCHOWA, 19 ARMII KRAJOWEJ AV., POLAND

** CZESTOCHOWA UNIVERSITY OF TECHNOLOGY, INSTITUTE OF MATERIALS SCIENCE, 42-200 CZĘSTOCHOWA, 19 ARMII KRAJOWEJ AV., POLAND

*** HOVE, EAST SUSSEX, UNITED KINGDOM

cooling rates (around 10^{-1} – 10^3 K/s) using suction- or injection-casting methods. In these methods, the liquid alloy is ejected or injected under high-pressure into a copper mould of a user-defined shape [7, 8]. The final sample can be produced in sizes of up to a few millimetres [9].

This work focuses on an investigation of the influence of additive elements on the soft magnetic properties and core losses in ribbon-shaped, multi-component $\text{Fe}_{61}\text{Co}_{10}\text{Y}_8\text{Me}_1\text{B}_{20}$ ferromagnetic alloys (where Me = W, Zr or Nb) in the as-quenched state.

2. Research methodology; studied materials

The components used in the production process were high-purity elements: Fe = 99.98, Co = 99.98, Y = 99.98, Zr = 99.99, Nb = 99.99 and W = 99.999; pure boron was added to the alloy in the form of a $\text{Fe}_{45.4}\text{B}_{54.6}$ alloy.

The ingots of $\text{Fe}_{61}\text{Co}_{10}\text{Y}_8\text{Me}_1\text{B}_{20}$ alloys (where Me = W, Zr or Nb) were obtained using arc-melting and then re-melted several times in order to ensure homogeneity of their polycrystalline structure. The samples of the investigated alloys were produced using a single-roller melt-spinning method.

Each liquid alloy was quenched on a rotating copper wheel, with a linear velocity of 30 m/s. The finished samples were of ribbon-form with thicknesses of approximately $30\ \mu\text{m}$ and widths of 3 mm. For all of the samples, the production process was performed under a protective argon atmosphere, which significantly reduced material oxidation. The microstructure of the samples was studied by means of a Bruker X-rays diffractometer equipped with a cobalt cathode Cu-K_α ($1.5418\ \text{\AA}$).

The saturation magnetization $\mu_0 M_s$, coercivity H_c and anisotropy field were measured (up to a magnetic field of 2 T) using a ‘LakeShore’ vibrating sample magnetometer (VSM). From measurements performed using a FERROTETER ferrometer, based on transformer method, the maximal magnetic permeability and dependence of core losses on the magnetizing field and frequency in a varying magnetic field were derived. All of these measurements were taken after de-magnetizing each sample.

3. Results and discussion

The X-ray diffraction patterns obtained for the investigated alloys are shown in Fig. 1.

The arrangement of atoms within amorphous materials is difficult to characterize due to the existing structural disorder. This explains why sharp, narrow lines (related with distance between atomic layers) cannot be observed in the X-ray diffraction patterns for amorphous alloys. In the X-ray diffraction patterns for the investigated alloys (shown in Fig. 1) only broad maxima can be observed; this confirms the amorphous structure of the obtained samples.

One of the most important parameters for electrotechnical applications of magnetic materials is the total value of the core losses during a reversal magnetization cycle. According to the theory the core losses consist of three factors:

$$P^{total} = P^{phys} + P^{class} + P^{exc} \quad (1)$$

where: P^{phys} – hysteresis loss, P^{class} – classical loss, P^{exc} – excess loss [10, 14].

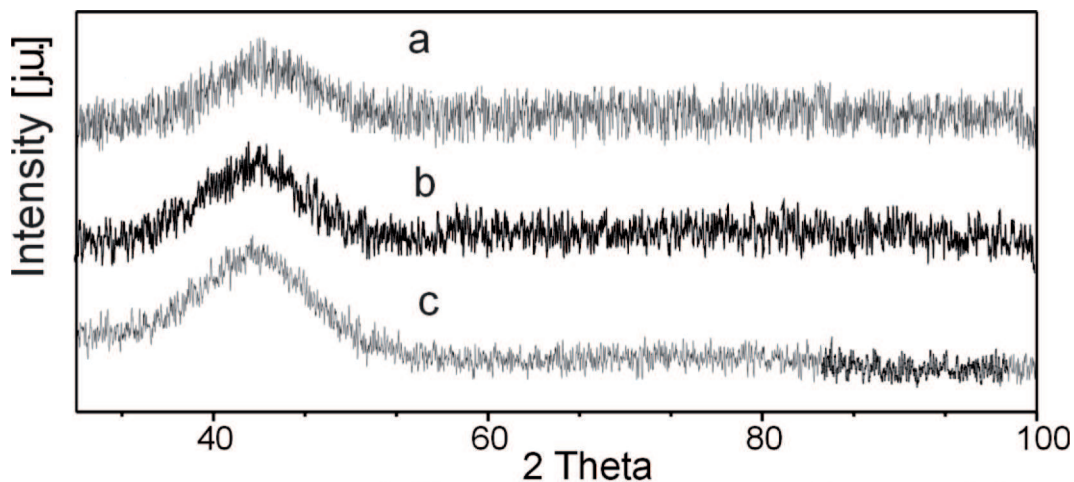


Fig. 1. X-ray diffraction patterns obtained for the investigated samples of $\text{Fe}_{61}\text{Co}_{10}\text{Y}_8\text{Me}_1\text{B}_{20}$ alloys, where Me= Nb (a), W (b) or Zr (c)

The measurements of core losses for the investigated alloys were performed on toroidal samples of amorphous ribbons, wound on quartz formers. For all of the investigated alloys, the diameter of the former and number of turns of the ribbon were the same, in order to compare precisely the values of core losses. The measurements were performed under the same conditions and parameters. The dependence of core losses on frequency at constant maximal magnetic induction ($B_{max} = 0.4$ T) are shown in Fig.2.

The theoretical matching and determination of the parameters was made on the basis of the dependence [14]:

$$P(f) = P^{hist} + P^{class} = k_1 f + k_2 f^2 \quad (2)$$

Where, for the alloy with the addition of:

$$\begin{aligned} \text{Nb } k_1 &= (2.18 \pm 0.09) 10^{-3}, k_2 = (1.77 \pm 0.09) 10^{-6}, \\ \text{W } k_1 &= (1.70 \pm 0.09) 10^{-3}, k_2 = (0.77 \pm 0.09) 10^{-6}, \\ \text{Zr } k_1 &= (2.45 \pm 0.09) 10^{-3}, k_2 = (1.30 \pm 0.09) 10^{-6} \end{aligned}$$

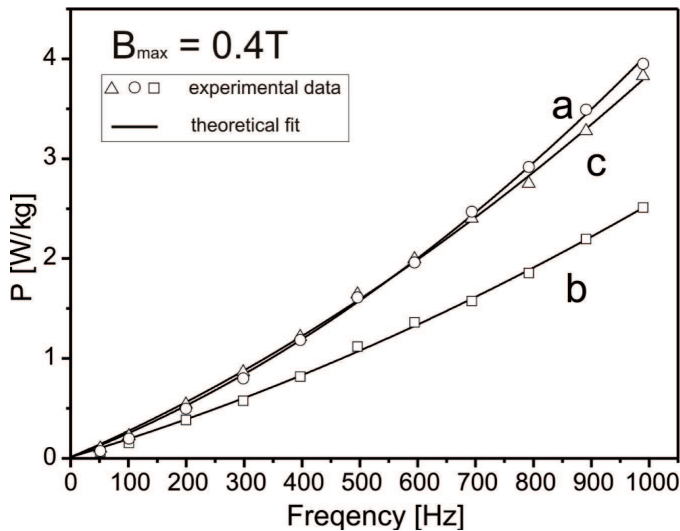


Fig. 2. Dependence of core losses on frequency for the $\text{Fe}_{61}\text{Co}_{10}\text{Y}_8\text{Me}_1\text{B}_2$ alloys, where: Me= Nb (a), W (b) or Zr (c)

From the aforementioned results, it can be seen that the addition of tungsten to the $\text{Fe}_{61}\text{Co}_{10}\text{Y}_8\text{Me}_1\text{B}_{20}$ alloy significantly reduced core losses compared to the other two alloys. The core losses present in the two remaining alloys are similar in the frequency range up to 700 Hz. Above 700 Hz, a small increase in core losses for the $\text{Fe}_{61}\text{Co}_{10}\text{Y}_8\text{Nb}_1\text{B}_{20}$ alloy can be observed.

On the basis of a theoretical fit of $P(f)$ dependence, the losses from hysteresis and on eddy currents were determined. Data obtained from the calculations were summarized in Table 1. On it's basis, it was found that the percentage of losses from hysteresis and on eddy current for the $\text{Fe}_{61}\text{Co}_{10}\text{Y}_8\text{Nb}_1\text{B}_{20}$ alloy are respectively 55% and 45%. For the other two alloys $\text{Fe}_{61}\text{Co}_{10}\text{Y}_8\text{W}_1\text{B}_{20}$ and $\text{Fe}_{61}\text{Co}_{10}\text{Y}_8\text{Zr}_1\text{B}_{20}$ the increase of losses from hysteresis, measured at frequencies from 50 Hz to 1000 Hz,

was observed. Their share was 71% and 65%, respectively.

On the basis of the performed studies, the investigated thin ribbons of $\text{Fe}_{61}\text{Co}_{10}\text{Y}_8\text{Me}_1\text{B}_{20}$ alloys (where Me = W, Zr or Nb) can be classified as excellent materials for medium-power transformers, working under low values of inductance.

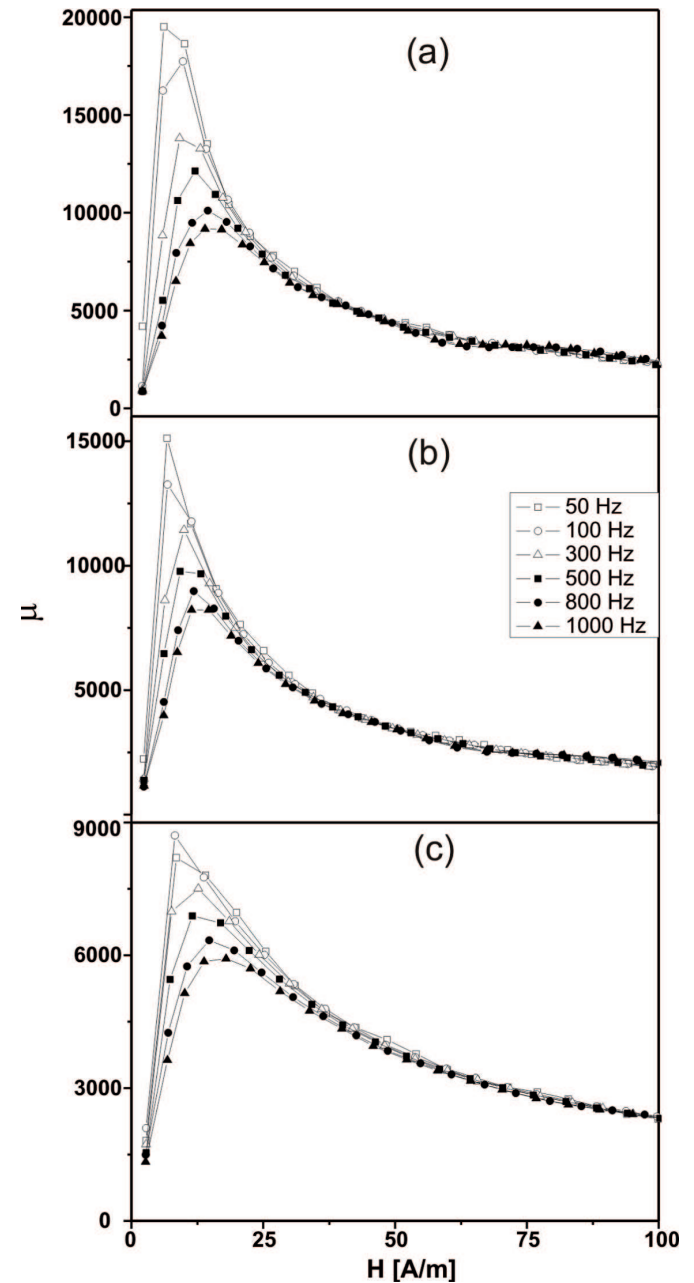


Fig. 3. Magnetic permeability for various frequencies of applied magnetizing field for the $\text{Fe}_{61}\text{Co}_{10}\text{Y}_8\text{Me}_1\text{B}_2$ alloys, where: Me = Nb (a), W (b) or Zr (c)

For example, commercially-produced ET 165-35 transformer sheets, for a frequency of 50 Hz and 0.4 T magnetic induction, exhibit a core loss of 0.105 W/kg [22]. The investigated in this article $\text{Fe}_{61}\text{Co}_{10}\text{Y}_8\text{W}_1\text{B}_{20}$

material, at a frequency of 50 Hz has a core losses at the level of 0.046 W/kg.

Another ‘commercially’ important factor for choosing a material suitable for medium-power transformers is the magnetic permeability of the alloy. Fig. 3. shows the dependence of the magnetic permeability on the applied magnetic field for all of the investigated alloys. The highest value of the magnetic permeability ($19,500 \pm 400$) was achieved for $Fe_{61}Co_{10}Y_8Nb_1B_{20}$ alloy, at a magnetic field of $(6.1 \pm 0,3)$ A/m. For the two remaining alloys, $Fe_{61}Co_{10}Y_8W_1B_{20}$ and $Fe_{61}Co_{10}Y_8Zr_1B_{20}$, the values of magnetic permeability were found to be 15,120 (at a magnetic field of $(6.7 \pm 0,3)$ A/m) and $(8,700 \pm 400)$ ((at $8.2 \pm 0,3$) A/m), respectively.

As it can be deduced from Figs. 2 and 3 show that, for all of the investigated alloys the increase in frequency of applied magnetic field produces the increase in the value of core losses and subsequent decrease in the magnetic permeability. The value of magnetic field at which the maximal permeability for the alloys was observed is slightly different for the investigated alloy (Fig. 4.).

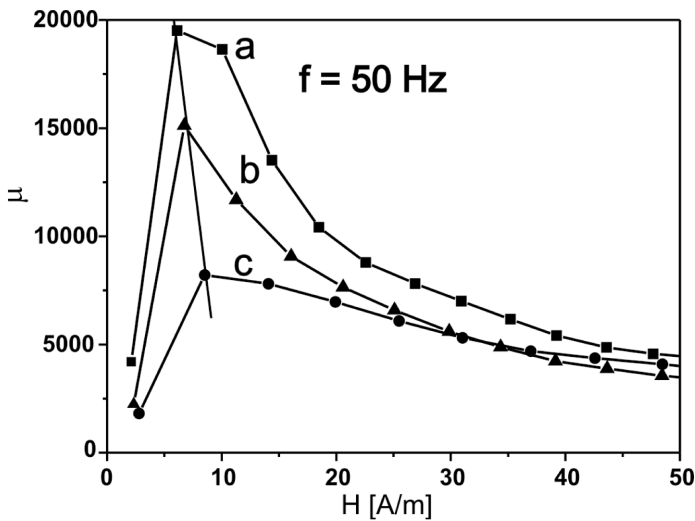


Fig. 4. Maximal magnetic permeability for the $Fe_{61}Co_{10}Y_8Me_1B_{20}$ alloys, measured at a frequency of 50 Hz, where: Me = Nb (a), W (b) or Zr (c)

It is connected with the change of coercivity field caused by use of additions to alloy composition. In the investigated alloy with the Nb addition the highest value of coercivity field ((101 ± 5) A/m) was observed. The maximum permeability, for this alloy, shifts towards lower magnetic fields, which may be associated with the fluctuations in the alloy composition and presence of areas with varying concentrations of iron. It should also added that niobium is a commonly used element to facilitate the obtaining of nanocrystalline structure. On the basis of research conducted by other authors [15] it was found that the alloys of Fe-Co-Nb-B type, crys-

tallize in the primary way. As is known in amorphous materials, in the production phase arise the so-called frozen embryos, whose rapid growth is limited by diffusing niobium on their borders from the amorphous matrix. As a result of this diffusion process it comes to the creation of the amorphous phase of different chemical composition, than the clusters of atoms forming the frozen embryos, which is consistent with the a model of primary crystallization. A small addition of W and Zr in the alloy reduces the coercivity field [16, 17], and for these materials the maximum permeability occurs at higher fields.

The soft magnetic properties of ferromagnetic materials can be found from measurements of the magnetic hysteresis loops. From analysis of the hysteresis loops, the saturation magnetization and the coercivity can be derived. The dependence $\mu_0 M = f(H)$ for all the investigated alloys is presented in Fig. 5. The saturation magnetization values were define for magnetic field of up to 2 T and posted in Table 1. In the case of an amorphous material with soft magnetic properties, the saturation state is usually achieved in a much lower magnetic field of under 1 T.

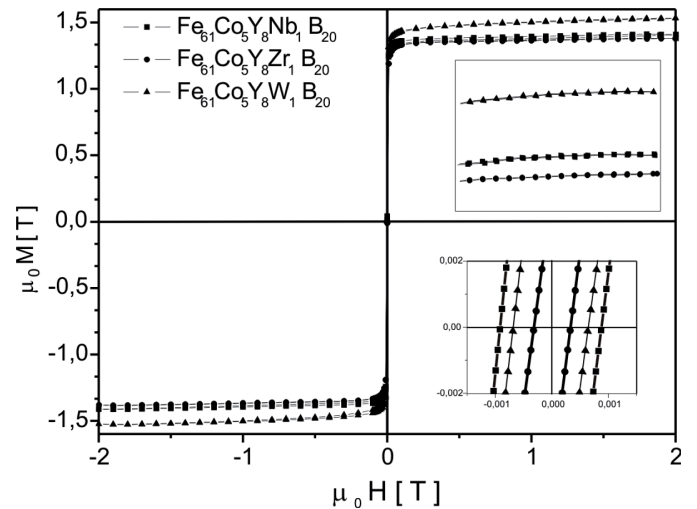


Fig. 5. Static hysteresis loops for the $Fe_{61}Co_{10}Y_8Me_1B_{20}$ alloys, in magnetic fields of up to 2 T, where Me = W, Zr or Nb

In high magnetic fields (above the value of the anisotropy field), the magnetic domain structure does not exist. The magnetization process in lower fields is related with rotation of the magnetization vector under the influence of structural defects, which are the source of short-distance stresses existing in micro-regions.

In even higher magnetic fields, if the saturation state is still not achieved, the magnetization process is related with diamagnetism of the closed electron shells and paramagnetism of the band electron [11-13].

The data obtained from analysis of the static hysteresis loops are presented in Table 1.

TABLE 1

Summary of parameters obtained for the investigated alloys: μ – maximal magnetic permeability, H_c - coercivity, $\mu_0 M_s$ – saturation magnetization, P – core losses, P_h – hysteresis loss, P_w – classical loss

| | H_c [A/m] | $\mu_0 M_s$ [T] | μ | | | | P [W/kg] dla $B_{max} = 0.4$ T | $P_{Total} =$ $P_h + P_w$ [W/kg] | P_h [W/kg] | P_w [W/kg] |
|-------------------------------|--------------------|------------------------|------------------------|----------------------|-----------------------|------------------------|-----------------------------------|--|------------------------|------------------------|
| | | | f = 50 Hz | H_{50Hz} [A/m] | f = 1000 Hz | H_{1000Hz} [A/m] | | | | |
| $Fe_{61}Co_{10}Y_8Nb_1B_{20}$ | 101 (± 5) | 1.41 (± 0.07) | 19500 (± 400) | 6.1 (± 0.3) | 9175 (± 400) | 13.97 (± 0.3) | 0.057 (± 0.002) | 3.96 (± 0.09) | 2.18 (± 0.09) | 1.78 (± 0.09) |
| $Fe_{61}Co_{10}Y_8W_1B_{20}$ | 61 (± 5) | 1.52 (± 0.07) | 15100 (± 400) | 6.7 (± 0.3) | 8221 (± 400) | 14.64 (± 0.3) | 0.046 (± 0.002) | 2.47 (± 0.09) | 1.70 (± 0.09) | 0.77 (± 0.09) |
| $Fe_{61}Co_{10}Y_8Zr_1B_{20}$ | 42 (± 5) | 1.38 (± 0.07) | 8700 (± 400) | 8.2 (± 0.3) | 5921 (± 400) | 17.94 (± 0.3) | 0.083 (± 0.002) | 3.75 (± 0.09) | 2.45 (± 0.09) | 1.30 (± 0.09) |

Saturation of the magnetization for the investigated alloys is high and falls within the range from $(1.38 \pm 0.07)T$ to $(1.52 \pm 0.07)T$. In accordance with the posted results in Tab. I it can be seen that for investigated alloys, saturation of the magnetization decreases with increasing radius of the exchanged atomic elements. That is described in dependence $W < Nb < Zr$ [18]. It is obvious that the value of saturation of the magnetization, in the alloys of metal-metalloid construction, is dependent on the exchange interactions which, in our case, occurs between a pair of Fe and Co magnetic elements. In the investigated alloys Co and Fe content is constant, so the deterioration of magnetic interactions between these elements must be caused by the addition of W, Zr or Nb atoms into the amorphous structure. On the basis of investigations of the magnetic properties, carried out by other authors for alloys with similar chemical compositions, it can be concluded that a small addition of W element, into the ferrimagnetic alloy, is beneficial for the improvement of so-called soft magnetic properties in particular, leads to increase of M_s [18, 19]. Insertion of 1 at.% of Me = Zr or Nb into the $Fe_{61}Co_{10}Y_8Me_1B_{20}$ alloy, reduces the value of the saturation of magnetization M_s , of more than one tenth, in comparison to M_s for $Fe_{61}Co_{10}Y_8W_1B_{20}$ alloy. Additionally shows that during the creation of electrotechnical materials, such as transformer cores, these components should be limited or completely eliminated from the alloy composition. The results of investigations on $Fe_{61}Co_{10}Zr_{2+x}Hf_{3-x}W_2Y_2B_{20}$ (where $x = 1, 2$ or 3) alloys presented by Nabialek et al [20] shows that increasing the content of Zr in this alloy system leads to a reduction in the M_s value. In another study, Kulik et al [15] had concluded, that the elimination of Nb, from the composition of $Fe_{76.5-x}Cu_1Nb_xSi_{13.5}B_9$ (where $x = 0, 1, 2, 3$) alloy, was beneficial for increasing M_s .

4. Conclusions

The single-roller melt-spinning method, used in this work, allowed the manufacture of fully amorphous ribbons of the $Fe_{61}Co_{10}Y_8Me_1B_{20}$ alloys (where: Me = W, Zr or Nb).

On the basis of the performed studies it was found that:

- the addition of 1 at.% of tungsten into the base alloy caused a decrease in the core losses and an increase in the saturation magnetization $\mu_0 M_s$ up to $(1.52 \pm 0.07)T$, in comparison with two other studied alloys;
- the smallest coercivity field (H_c) showed $Fe_{61}Co_{10}Y_8Zr_1B_{20}$ alloy;
- the maximal magnetic permeability, $\mu_{max}(50\text{ Hz}) = (19.500 \pm 400)$, was observed for the $Fe_{61}Co_{10}Y_8Nb_1B_{20}$ alloy.

It can be seen that each of additives had a different influence on the soft magnetic properties of the resulting alloy. However, for application in modern medium-power transformer magnetic cores, the best additive has been found to be tungsten, as it improved the most important electro-technical parameters of the material.

These alloys have better electrical characteristics than the commercially used transformer Fe-Si sheets [21, 22].

REFERENCES

- [1] M.E. McHenry, M.A. Willard, D.E. Laughlin, Prog. Mater. Sci. **44**, 291-433 (1999).
- [2] M. Nabiałek, J. Zbrozczyk, W. Ciurzyńska, J. Olszewski, S. Lesz, P. Brągiel, J. Gondro, K. Sobczyk, A. Łukiewska, J. Świerczek, P. Pietrusiewicz, Microstructure, some magnetic and mechanical properties of amorphous $Fe_{61}Co_{10}Zr_{2.5}W_2Hf_{2.5}Y_2B_{20}$ plates, Archives of Metallurgy and Materials **55**, 349-357 (2010).

- [3] H. Liu, Ch. Yin, X. Miao, Z. Han, D. Wang, Y. Du, *J. of Alloys and Compounds* **466**, 246 (2008).
- [4] R.J. Hasegawa, *Magn. Magn. Mater.* **240-245**, 215-216 (2000).
- [5] A. Inoue, *Acta Materialia* **48**, 279 (2000).
- [6] D.Y. Liu, W.S. Sun, H.F. Zhang, Z.Q. Hu, *Intermetallics* **12**, 1149 (2004).
- [7] P. Pawlik, M. Nabiałek, E. Żak, J. Zbroszczyk, J.J. Wysocki, J. Olszewski, K. Pawlik, *Archiwum nauki materiałach* **25**, 177 (2004).
- [8] H.S. Chen, C.E. Miller, *Review of Scientific Instruments* **41**, 1237 (1970).
- [9] A. Inoue, Z. Tao, *Materials Transactions, Japan Institute of Metals* **36**, 1184 (1995).
- [10] G. Bertotti, *Hysteresis in Magnetism*, Academic Press, San Diego, 1998.
- [11] H. Kronmüller, *Magnetization Processes and the Microstructure in Amorphous Metals*, *J. de Phys.* **41**, 518 (1980).
- [12] T. Holstein, H. Primakoff, *Magnetization near saturation in polycrystalline ferromagnet*, *Phys. Rev.* **59**, 388-394 (1941).
- [13] A.H. Morrish, *Fizyczne podstawy magnetyzmu*, 366-367 PWN Warszawa 1970.
- [14] J. Kuryłowicz, *Badania materiałów magnetycznych*, 283-286 WNT Warszawa 1962.
- [15] T. Kulik, *Nanokrystaliczne materiały magnetycznie miękkie otrzymane przez krystalizację szkiełmetalicznych*, Oficyna Wydawnicza Politechniki Warszawskiej, Warszawa (1998).
- [16] A. Makino, T. Bitoh, A. Kojima, A. Inoue, T. Masumoto, *Materials Science and Engineering* **A304-306**, 1083-1086 (2001).
- [17] X.M. Huang, C.T. Chang, Z.Y. Chang, A. Inoue, J.Z. Jiang, *Materials Science and Engineering A* **527**, 1952-1956 (2010).
- [18] M. Nabiałek, M. Szota, M. Dośpiał, P. Pietrusiewicz, S. Walters, *J. of Mag. and Magnet. Mater.* **322**, 3377-3380 (2010).
- [19] D.Y. Liu, W.S. Sun, A.M. Wang, H.F. Zhang, Z.Q. Hu, *J. Alloys Compd* **370**, 249-253 (2004).
- [20] M. Nabiałek, M. Dospiał, M. Szota, J. Olszewski, S. Walters, *J. Alloys Compd.* **509S**, 155-S160 (2011).
- [21] S. Azarewicz, D. Gaworska, B. Weglinski, *Zeszyty Problemowe – Maszyny Elektryczne* **No 72**, 129 (2005).
- [22] www.stalprodukt.com.pl